NIH Public Access
Author Manuscript
Nature. Author manuscript; available in PMC 2014 June 05.

Published in final edited form as:
Nature. ; 485(7399): 512–516. doi:10.1038/nature11087.

Apolipoprotein E controls cerebrovascular integrity via cyclophilin A

R. D. BELL[1,2], **E. A. WINKLER**[1], **I. SINGH**[1], **A. P. SAGARE**[1], **R. DEANE**[1], **Z. WU**[1], **D. M. HOLTZMAN**[3], **C. BETSHOLTZ**[4], **A. ARMULIK**[4,5], **J. SALLSTROM**[1], **B. C. BERK**[2], and **B. V. ZLOKOVIC**[1,6]

[1]Center for Neurodegenerative and Vascular Brain Disorders, University of Rochester Medical Center, Rochester, NY [2]Aab Cardiovascular Research Institute, University of Rochester Medical Center, Rochester, NY [3]Department of Neurology, Hope Center for Neurological Disorders, Knight Alzheimer's Disease Research Center, Washington University School of Medicine, St. Louis, MO [4]Division of Vascular Biology, Department of Medical Biochemistry and Biophysics, Karolinska Institutet, Stockholm, Sweden [5]Institute of Neuropathology, University Hospital Zürich, Zürich, Switzerland [6]Center for Neurodegeneration and Regeneration Zilkha Neurogenetic Institute and Department of Physiology and Biophysics, University of Southern California, Keck School of Medicine CA

Abstract

Human apolipoprotein E has three isoforms: APOE2, APOE3 and APOE4[1]. *APOE4* is a major genetic risk factor for Alzheimer's disease[2, 3] and is associated with Down's syndrome dementia and poor neurological outcome after traumatic brain injury and haemorrhage[3]. Neurovascular dysfunction is present in normal *APOE4* carriers[4, 5, 6] and individuals with*APOE4*-associated disorders[3, 7, 8, 9, 10]. In mice, lack of *Apoe* leads to blood–brain barrier (BBB) breakdown[11, 12], whereas *APOE4* increases BBB susceptibility to injury[13]. How *APOE* genotype affects brain microcirculation remains elusive. Using different APOE transgenic mice, including mice with ablation and/or inhibition of cyclophilin A (CypA), here we show that expression of APOE4 and lack of murine Apoe, but not APOE2 and APOE3, leads to BBB breakdown by activating a proinflammatory CypA–nuclear factor-κB–matrix-metalloproteinase-9 pathway in pericytes. This, in turn, leads to neuronal uptake of multiple blood-derived neurotoxic proteins, and microvascular and cerebral blood flow reductions. We show that the vascular defects in *Apoe*-deficient and *APOE4*-expressing mice precede neuronal dysfunction and can initiate neurodegenerative changes. Astrocyte-secreted APOE3, but not APOE4, suppressed the CypA–nuclear factor-κB–matrix-metalloproteinase-9 pathway in pericytes through a lipoprotein receptor. Our data suggest

Address for Correspondence: Berislav V. Zlokovic, M.D., Ph.D., Center for Neurodegeneration and Regeneration, Zilkha Neurogenetic Institute, University of Southern California, Keck School of Medicine, 1501 San Pablo St. Los Angeles, CA 90089, zlokovic@usc.edu.

Author Contributions RDB designed and performed experiments, analyzed data and contributed to writing the paper; EAW designed and performed experiments; IS performed experiments; APS performed CBF experiments; RD designed experiments; ZW gathered pilot data; DMH provided guidance and edited the paper; CB designed experiments and edited the paper, AA performed pilot cadaverine studies; JS generated pilot data; BCB provided guidance and edited the paper; BVZ designed experiments, analyzed data and wrote the paper.

NIH-PA Author Manuscript
NIH-PA Author Manuscript
NIH-PA Author Manuscript

NIH-PA Author Manuscript

NIH-PA Author Manuscript

NIH-PA Author Manuscript

that CypA is a key target for treating APOE4-mediated neurovascular injury and the resulting neuronal dysfunction and degeneration.

Astrocytes are a major source of APOE in the brain[2]. Importantly, astrocyte-secreted molecules transduce signals to brain microvessels acting on pericytes[7, 14, 15]. To understand the effects of APOE on brain microcirculation we studied mice with targeted replacement of murine Apoe with each human APOE isoform (TR-*APOE*)[16], mice lacking murine Apoe (*Apoe*$^{-/-}$), mice expressing each human APOE isoform under control of the astrocyte-specific glial fibrillary acidic protein (GFAP) promoter on an Apoe-null background, and *Apoe*$^{-/-}$ and *APOE4* transgenic mice with ablation and/or pharmacological inhibition of CypA (see Supplementary Information). In search of molecules that could mediate BBB dysfunction in *Apoe*$^{-/-}$ and *APOE4* mice, we focused on the proinflammatory cytokine CypA, previously demonstrated to have deleterious effects on the vascular system in *Apoe*$^{-/-}$ mice with aortic aneurysms and atherosclerosis[17, 18].

Using multiphoton microscopy of tetramethylrhodamine-conjugated dextran (TMR-dextran)[14], we show an intact BBB in TR-*APOE2* and TR-*APOE3* mice and a leaky BBB in TR-*APOE4* and *Apoe*$^{-/-}$ mice (Fig. 1a and Supplementary Fig. 1a, b), suggesting that APOE2, APOE3 and murine Apoe effectively maintain the BBB, whereas APOE4 promotes BBB disruption. These findings have been replicated in mice expressing each human APOE isoform under control of the GFAP promoter (not shown). Notably, genetic ablation of CypA (encoded by *Ppia*) eliminated BBB damage in *Apoe*$^{-/-}$ *Ppia*$^{-/-}$ mice (Fig. 1a and Supplementary Fig. 1a, b).

Compared to littermate controls, TR- or GFAP-*APOE2* and -*APOE3* mice, *Apoe*$^{-/-}$ and *APOE4* mice had five- to sixfold higher CypA levels in cerebral microvessels (Fig. 1b and Supplementary Fig. 1c, d), mainly because of an increased CypA expression in pericytes (Fig. 1c and Supplementary Fig. 1e). CypA levels in microvessel-depleted brain were not affected by APOE (Supplementary Fig. 1f). These data suggest that APOE2, APOE3 and murine Apoe, but not APOE4, effectively maintain physiological CypA levels in brain microvessels by controlling CypA expression in pericytes. To determine whether BBB disruption in *APOE4* mice can be corrected with cyclosporine A, a drug that binds intracellular CypA and inhibits its effects[19], we treated TR-*APOE4* and GFAP-*APOE4* mice with a low dose of cyclosporine A previously shown not to cause systemic or central nervous system toxicity. Cyclosporine A accumulates in brain microvessels, but does not cross the BBB[20]. In *APOE4* mice cyclosporine A eliminated BBB disruption (Fig. 1a and Supplementary Fig. 1a, b) and neuronal accumulation of systemically administered cadaverine[15] (Supplementary Fig. 1g), indicating that BBB changes are reversible and CypA can be therapeutically targeted to correct*APOE4*-induced BBB breakdown.

To understand better the pathological implications of BBB breakdown, we studied leakage of endogenous blood-derived proteins in the brain. As shown in the hippocampus, 18-month-old GFAP-*APOE3* and control mice had negligible extravascular accumulation of serum IgG in contrast to GFAP-*APOE4* and *Apoe*$^{-/-}$ mice (Supplementary Fig. 2a, b). *Ppia* genetic deletion eliminated IgG extravascular deposits (Supplementary Fig. 2a, b) and neuronal accumulation in *Apoe*$^{-/-}$ and *APOE4* mice (Fig. 1d). Cyclosporine A diminished

NIH-PA Author Manuscript

NIH-PA Author Manuscript

NIH-PA Author Manuscript

IgG leakage by ~80% in TR-*APOE4* or GFAP-*APOE4* mice (Supplementary Fig. 2c) and inhibited neuronal accumulation of blood-derived thrombin and fibrin (Fig. 1e), consistent with restoration of the BBB. *APOE4* mice had numerous brain perivascular fibrin and haemosiderin foci (Supplementary Fig. 2d–f) and elevated thrombin levels that were normalized with cyclosporine A (Supplementary Fig. 2g, h). Thrombin is neurotoxic[21], fibrin accelerates neurovascular damage[22] and haemosiderin generates reactive oxygen species[23], thus implicating multiple potential BBB-derived sources of injury.

To elucidate the molecular mechanisms underlying CypA-mediated BBB breakdown we studied matrix metalloproteinases (MMP)2 and MMP9 (gelatinases), which are activated by CypA in the vessel wall in a mouse model of aortic aneurism[17]. Gelatinases disrupt the BBB by degrading the capillary basement membrane and tight-junction proteins[7, 24]. Multiphoton microscopy of DQ-gelatin[25] revealed an increase in cerebrovascular gelatinase activity in *Apoe*$^{-/-}$ *Ppia*$^{+/+}$ and TR-*APOE4* mice compared with controls, TR-*APOE2* and TR-*APOE3* mice (Fig. 2a, b). Gelatin zymography of brain tissue demonstrated an increase in pro-MMP9 and activated MMP9, but not MMP2, in *Apoe*$^{-/-}$ and TR-*APOE4* mice (Fig. 2c), which correlated with the appearance of MMP9-positive pericytes (Fig. 2d and Supplementary Fig. 3a, b). To establish causality and demonstrate that increased MMP9 activity does not only correlate with, but is required for, BBB breakdown in *Apoe*$^{-/-}$ and TR-*APOE4* mice, we studied the effects of pharmacological inhibition of MMP9 *in vivo* with 2-[[(4-phenoxyphenyl)sulfonyl]methyl]-Thiirane (SB-3CT), an MMP9 inhibitor, and of MMP9 and MMP2 silencing by short interfering (si)RNA administration into the hippocampus, as reported[26]. SB-3CT eliminated MMP9 gelatinase activity (Fig. 2b, c) and reversed the leaky BBB phenotype (Supplementary Fig. 4a) in both mouse lines. Similarly, MMP9, but not MMP2, silencing reversed the BBB phenotype in TR-*APOE4* mice (Supplementary Fig. 4b). Similar results were obtained with *siMmp9* treatment in *Apoe*$^{-/-}$ mice (not shown).

Consistent with MMP9 activation, several MMP9 substrates including collagen IV and tight-junction proteins ZO-1 (also known as Tjp1), occludin and claudin 5, which are required for normal BBB integrity[7, 24] were reduced in brain microvessels in young *Apoe*$^{-/-}$ and *APOE4* mice, indicating BBB breakdown (Fig. 2e and Supplementary Fig. 3c–f). SB-3CT (Supplementary Fig. 4c) and *siMMP-9*, but not *siMMP-2* or control siRNA, normalized the levels of tight-junction and basement-membrane proteins in *APOE4* (Supplementary Fig. 4b) and *Apoe*$^{-/-}$ mice (not shown). These data explain how MMP9 inhibition permits reversal of BBB disruption in *Apoe*$^{-/-}$ and *APOE4* mice at a molecular level. Notably, genetic deletion of *Ppia* or cyclosporine A substantially inhibited gelatinase/MMP9 activity (Fig. 2a–c) and restored the basement-membrane and tight-junction proteins in *Apoe*$^{-/-}$ *Ppia*$^{-/-}$ and TR-*APOE4* mice (Fig. 2e and Supplementary Figs 3c–f, 4c).

Nuclear-factor-κB (NF-κB) transcriptionally activates MMP9 in cerebral vessels, causing BBB breakdown[24]. Consistent with findings that CypA at pathophysiological levels activates NF-κB and the NF-κB–MMP9 pathway[18, 24, 27], we found NF-κB nuclear translocation in brain capillary pericytes in *Apoe*$^{-/-}$ and *APOE4* mice (Supplementary Fig. 5a, b). In both *Apoe*$^{-/-}$ and *APOE4* mice, NF-κB nuclear translocation was inhibited by *Ppia* gene deletion and/or cyclosporine A (Supplementary Fig. 5a, b).

NIH-PA Author Manuscript

NIH-PA Author Manuscript

NIH-PA Author Manuscript

To establish the causality between NF-κB activation, increased gelatinase activity and BBB breakdown, we treated *Apoe*$^{-/-}$ and *APOE4* mice with pyrrolidine dithiocarbamate (PDTC), an inhibitor of NF-κB nuclear translocation. In *Apoe*$^{-/-}$ and *APOE4* mice, PDTC markedly reduced MMP9 activation (Fig. 2b, c and Supplementary Fig. 3b) and reversed the leaky BBB phenotype (Supplementary Fig. 4a). Consistent with these data, NF-κB inhibition in the hippocampus by silencing *Rela*, which encodes the p65 subunit of NF-κB, inhibited MMP9 and reversed the BBB phenotype in *APOE4* mice (Supplementary Fig. 4c). Similar results were obtained by silencing *Rela* in *Apoe*$^{-/-}$ mice (not shown). Our findings therefore clearly establish that each of the molecules studied (that is, CypA, NF-κB and MMP9) have important and required roles in BBB disruption in *Apoe*$^{-/-}$ and *APOE4* mice.

Consistent with reports that chronic BBB breakdown leads to microvascular reductions[7, 14, 22], we found microvascular degeneration in *APOE4* and *Apoe*$^{-/-}$ mice, including DNA fragmentation in pericytes and endothelial cells (Supplementary Fig. 6a), diminished pericyte coverage (Supplementary Fig. 5b, c) and reductions in microvascular length (Fig. 3a and Supplementary Fig. 6d), which correlated with the degree of BBB breakdown (Supplementary Fig. 6e) and regional cerebral blood flow (CBF) reductions (Fig. 3b and Supplementary Table 1). Notably, *Ppia* deletion and cyclosporine A, SB-3CT or PDTC normalized microvascular reductions in *Apoe*$^{-/-}$ and *APOE4* mice (Fig. 3a and Supplementary Fig. 6c). *Ppia* deletion also normalized CBF reductions in *Apoe*$^{-/-}$ mice (Fig. 3b).

Given that CypA expression and NF-κB and MMP9 activation are increased in pericytes in *Apoe*$^{-/-}$ and *APOE4* mice, we next studied which low-density lipoprotein (LDL)/APOE receptor[1] in pericytes regulates CypA in response to astrocyte-derived APOE. After confirming the specificity of our siRNA reagents (Supplementary Fig. 7), we showed by quantifying the effects of siRNA inhibition (Fig. 4a and Supplementary Fig. 8a–d) and by administering antibodies to block the function of specific LDL receptors (Supplementary Fig. 8e–g) that astrocyte-derived APOE3 and murine Apoe require low-density lipoprotein receptor-related protein 1 (LRP1) to maintain CypA synthesis within a physiological range. Adenoviral-mediated re-expression of a human *LRP1* minigene rescued the ability of APOE3 to downregulate *Ppia* mRNA (Fig. 4a) and protein (Supplementary Fig. 8b) in pericytes with siRNA-induced LRP1 knockdown. By imaging APOE/LRP1 proximity ligation in pericytes we demonstrated that APOE3 (Fig. 4b) and murine Apoe (not shown) bind with high affinity to LRP1, whereas the APOE4–LRP1 interaction was barely detectable (Fig. 4b). Together these data explain at the molecular level why APOE4 is unable to properly regulate physiologic CypA levels, which is consistent with previously reported statistically insignificant interactions of APOE4 with LRP1 in cerebral microvessels and at the BBB *in vivo*[28].

Ppia silencing, cyclosporine A and astrocyte-derived APOE3, but not APOE4, inhibited NF-κB nuclear translocation in *Apoe*$^{-/-}$ pericytes (Supplementary Fig. 9a), as *in vivo*. By using *siLrp1* silencing, cyclosporine A or PDTC, we showed that LRP1 is required for APOE3-mediated inhibition of NF-κB-dependent MMP9 activation and transcriptional suppression[24] (Supplementary Fig. 9). APOE4 did not have an effect on MMP9 in pericytes, consistent with its barely detectable binding to LRP1 (Fig. 4b). *In vivo*, LRP1 inhibition in *APOE3*

NIH-PA Author Manuscript

NIH-PA Author Manuscript

NIH-PA Author Manuscript

mice through siRNA administration in the hippocampus[26] reproduced vascular phenotypes seen in *APOE4* mice, including elevated CypA and MMP9 levels and increased CypA and MMP9 expression in pericytes (Fig. 4c and Supplementary Fig. 10a, b), and BBB breakdown (Fig. 4d). As expected, LRP1 inhibition in mice with *Ppia* genetic deletion did not influence MMP9 expression in pericytes (Supplementary Fig. 10d) or BBB integrity (Supplementary Fig. 10d). Together, these data clearly implicate APOE3/LRP1-mediated CypA regulation in pericytes, conferring APOE3 isoform-specific protection of the BBB (Fig. 4e).

Vascular defects in *Apoe*$^{-/-}$ and *APOE4* mice were detectable at 2 weeks of age, including leakage of dextran (Fig. 5a) and serum IgG (Supplementary Fig. 11a), and reductions in tight-junction and basement-membrane proteins, pericyte coverage, capillary length and regional CBF, which progressively increased with age (Fig. 2e and Supplementary Figs 11b–e, 12 and Supplementary Table 1). We next asked whether vascular damage precedes neuronal changes in *Apoe*$^{-/-}$ mice[29], and neuronal and synaptic dysfunction in *APOE4* mice[2]. Cortical activity determined *in vivo* by voltage-sensitive dye (VSD) imaging indicated normal time-lapse imaging profiles in 2-week-old*Apoe*$^{-/-}$ and *APOE4* mice (Fig. 5b and Supplementary Fig. 13a, b) and normal neuritic density and levels of pre-synaptic and post-synaptic proteins (Supplementary Fig. 14a–d). At 4 months of age, however, *Apoe*$^{-/-}$ and *APOE4* mice showed a lower amplitude of the VSD signal, longer time-to-peak and a slower duration of the spreading of depolarization (Fig. 5c, d), which was accompanied by age-dependent reductions in neuritic density and pre-synaptic and post-synaptic proteins (Supplementary Fig. 14a–f). These data indicate that *Apoe*$^{-/-}$ and *APOE4* mice develop vascular defects before neuronal and synaptic changes occur. Cyclosporine A, PDTC and SB-3CT improved functional and structural neuronal changes in *Apoe*$^{-/-}$ and *APOE4* mice (Fig. 5e and Supplementary Fig. 15), indicating that normalization of BBB integrity through inhibition of the CypA–NF-κB–MMP9 pathway is required for neuronal and synaptic repair.

Understanding the contribution of APOE4 to the pathogenesis of Alzheimer's disease may be one of the most important avenues to a new therapy. Neurovascular dysfunction and BBB defects have been shown in Alzheimer's disease [7, 30]. The findings from this study indicating that abnormal vessels and pericytes can be involved provide an alternative way of thinking about Alzheimer's disease and neurological disorders affected by APOE4. Our findings demonstrate that APOE maintains cerebrovascular integrity necessary for normal neuronal function by regulating the CypA–NF-κB–MMP9 pathway in pericytes in an isoform-specific manner (Fig. 4e). We also show that CypA is a key target for treating APOE4-mediated neurovascular defects and the resulting neuronal dysfunction.

METHODS SUMMARY

Animals

Apoe$^{-/-}$, GFAP-*APOE* mice on murine apoE null background and *Ppia*$^{-/-}$ mice were acquired from Jackson Laboratories. TR-*APOE* mice were generated as previously described[16]. The *Ppia*$^{-/-}$ mice were crossed to the *Apoe*$^{-/-}$ and TR-*APOE4* mice to generate the *Apoe*$^{-/-}$ *Ppia*$^{-/-}$ and TR-*APOE4 Ppia*$^{-/-}$ mice used in the present study. Mice were

NIH-PA Author Manuscript

NIH-PA Author Manuscript

NIH-PA Author Manuscript

housed in plastic cages on a 12 h light cycle with ad libitum access to water and a standard laboratory diet. All studies were performed in accordance with the University of Rochester Institutional Animal Care and Use Committee using National Institute of Health guidelines. All lines were maintained on a C57Bl6 background. No significant phenotypic differences were found between littermate control animals.

Pharmacological inhibition

In some studies, *APOE4* or *Apoe*$^{-/-}$ mice were treated for 7 consecutive days with a low intraperitoneal non-toxic dose of cyclosporine A (Sigma, 30024-25; 10 mg/kg/day for 3 days followed by 5 mg/kg/day for 4 days), or pyrrolidine dithiocarbamate (PDTC, 100 mg/kg/day) or SB-3CT (25 mg/kg/day).

In vivo si*RNA* infusion

si*RNA*-mediated LRP1, MMP-9, MMP-2 and RELA knockdown was performed as previously described[26].

Blood-brain barrier permeability assays

In vivo multiphoton imaging of TMR-conjugated dextran and detection of endogenous IgG, fibrin, thrombin and Prussian blue deposits in brain tissue was performed as previously described[14]. Detection of neuronal uptake of systemically administered Alexa fluor 555-conjugated cadaverine was performed as described[15].

Stastical analysis

Data were analyzed by multifactorial analysis of variance (ANOVA) followed by Tukey posthoc tests and Pearson's correlation analysis using GraphPad Prism 3.0 software. A p value less than 0.05 was considered statistically significant in all studies.

A complete description of all experiments performed and associated references are available in the Supplemental Materials and Methods section.

Supplementary Material

Refer to Web version on PubMed Central for supplementary material.

Acknowledgments

We would like to thank the National Institutes of Health for grants R37NS34467(BVZ); R37AG23084(BVZ); RO1AG039452(BVZ); and R37AG13956(DMH) used to support this study.

References

1. Mahley RW, Weisgraber KH, Huang Y. Apolipoprotein E: structure determines function, from atherosclerosis to Alzheimer's disease to AIDS. J Lipid Res. 2009; 50 (Suppl):S183–188. [PubMed: 19106071]
2. Kim J, Basak JM, Holtzman DM. The role of apolipoprotein E in Alzheimer's disease. Neuron. 2009; 63:287–303. [PubMed: 19679070]
3. Verghese PB, Castellano JM, Holtzman DM. Apolipoprotein E in Alzheimer's disease and other neurological disorders. Lancet Neurol. 2011; 10:241–252. [PubMed: 21349439]

NIH-PA Author Manuscript

NIH-PA Author Manuscript

NIH-PA Author Manuscript

4. Thambisetty M, Beason-Held L, An Y, Kraut MA, Resnick SM. APOE epsilon4 genotype and longitudinal changes in cerebral blood flow in normal aging. Arch Neurol-Chicago. 2010; 67:93–98. [PubMed: 20065135]
5. Sheline YI, et al. APOE4 allele disrupts resting state fMRI connectivity in the absence of amyloid plaques or decreased CSF Abeta42. J Neurosci. 2010; 30:17035–17040. [PubMed: 21159973]
6. Reiman EM, et al. Functional brain abnormalities in young adults at genetic risk for late-onset Alzheimer's dementia. Proc Natl Acad Sci USA. 2004; 101:284–289. [PubMed: 14688411]
7. Zlokovic BV. Neurovascular pathways to neurodegeneration in Alzheimer's disease and other disorders. Nature Rev Nsci. 2011; 12:723–738.
8. Snowdon DA, et al. Brain infarction and the clinical expression of Alzheimer disease. The Nun Study. JAMA. 1997; 277:813–817. [PubMed: 9052711]
9. Vermeer SE, et al. Silent brain infarcts and the risk of dementia and cognitive decline. N Engl J Med. 2003; 348:1215–1222. [PubMed: 12660385]
10. Ruitenberg A, et al. Cerebral hypoperfusion and clinical onset of dementia: the Rotterdam Study. Ann Neurol. 2005; 57:789–794. [PubMed: 15929050]
11. Methia N, et al. ApoE deficiency compromises the blood brain barrier especially after injury. Mol Med. 2001; 7:810–815. [PubMed: 11844869]
12. Hafezi-Moghadam A, Thomas KL, Wagner DD. ApoE deficiency leads to a progressive age-dependent blood-brain barrier leakage. Am J Physiol Cell Physiol. 2007; 292:C1256–1262. [PubMed: 16870825]
13. Nishitsuji K, Hosono T, Nakamura T, Bu G, Michikawa M. Apolipoprotein E regulates the integrity of tight junctions in an isoform-dependent manner in an in vitro blood-brain barrier model. J Bio Chem. 2011; 286:17536–17542. [PubMed: 21471207]
14. Bell RD, et al. Pericytes control key neurovascular functions and neuronal phenotype in the adult brain and during brain aging. Neuron. 2010; 68:409–427. [PubMed: 21040844]
15. Armulik A, et al. Pericytes regulate the blood-brain barrier. Nature. 2010; 468:557–561. [PubMed: 20944627]
16. Sullivan PM, et al. Reduced levels of human apoE4 protein in an animal model of cognitive impairment. Neurobio Aging. 2011; 32:791–801.
17. Satoh K, et al. Cyclophilin A enhances vascular oxidative stress and the development of angiotensin II-induced aortic aneurysms. Nat Med. 2009; 15:649–656. [PubMed: 19430489]
18. Jin ZG, et al. Cyclophilin A is a proinflammatory cytokine that activates endothelial cells. Arterioscler Thromb Vasc Biol. 2004; 24:1186–1191. [PubMed: 15130913]
19. Handschumacher RE, Harding MW, Rice J, Drugge RJ, Speicher DW. Cyclophilin: a specific cytosolic binding protein for cyclosporin A. Science. 1984; 226:544–547. [PubMed: 6238408]
20. Begley DJ, et al. Permeability of the blood-brain barrier to the immunosuppressive cyclic peptide cyclosporin A. J Neurochem. 1990; 55:1222–1230. [PubMed: 2398356]
21. Grammas P. Neurovascular dysfunction, inflammation and endothelial activation: implications for the pathogenesis of Alzheimer's disease. J Neuroinflammation. 2011; 8:26. [PubMed: 21439035]
22. Paul J, Strickland S, Melchor JP. Fibrin deposition accelerates neurovascular damage and neuroinflammation in mouse models of Alzheimer's disease. J Exp Med. 2007; 204:1999–2008. [PubMed: 17664291]
23. Zhong Z, et al. Activated protein C therapy slows ALS-like disease in mice by transcriptionally inhibiting SOD1 in motor neurons and microglia cells. J Clin Invest. 2009; 119:3437–3449. [PubMed: 19841542]
24. Candelario-Jalil E, et al. Matrix metalloproteinases are associated with increased blood-brain barrier opening in vascular cognitive impairment. Stroke. 2011; 42:1345–1350. [PubMed: 21454822]
25. Garcia-Alloza M, et al. Matrix metalloproteinase inhibition reduces oxidative stress associated with cerebral amyloid angiopathy in vivo in transgenic mice. J Neurochem. 2009; 109:1636–1647. [PubMed: 19457117]

NIH-PA Author Manuscript

NIH-PA Author Manuscript

NIH-PA Author Manuscript

26. Jaeger LB, et al. Testing the neurovascular hypothesis of Alzheimer's disease: LRP-1 antisense reduces blood-brain barrier clearance, increases brain levels of amyloid-beta protein, and impairs cognition. J Alz Dis. 2009; 17:553–570.

27. Yang Y, Lu N, Zhou J, Chen ZN, Zhu P. Cyclophilin A up-regulates MMP-9 expression and adhesion of monocytes/macrophages via CD147 signalling pathway in rheumatoid arthritis. Rheumatology. 2008; 47:1299–1310. [PubMed: 18567920]

28. Deane R, et al. apoE isoform-specific disruption of amyloid beta peptide clearance from mouse brain. J Clin Invest. 2008; 118:4002–4013. [PubMed: 19033669]

29. Masliah E, et al. Neurodegeneration and cognitive impairment in apoE-deficient mice is ameliorated by infusion of recombinant apoE. Brain Res. 1997; 751:307–314. [PubMed: 9099820]

30. Zipser BD, et al. Microvascular injury and blood–brain barrier leakage in Alzheimer's disease. Neurobiol Aging. 2007; 28:977–986. [PubMed: 16782234]

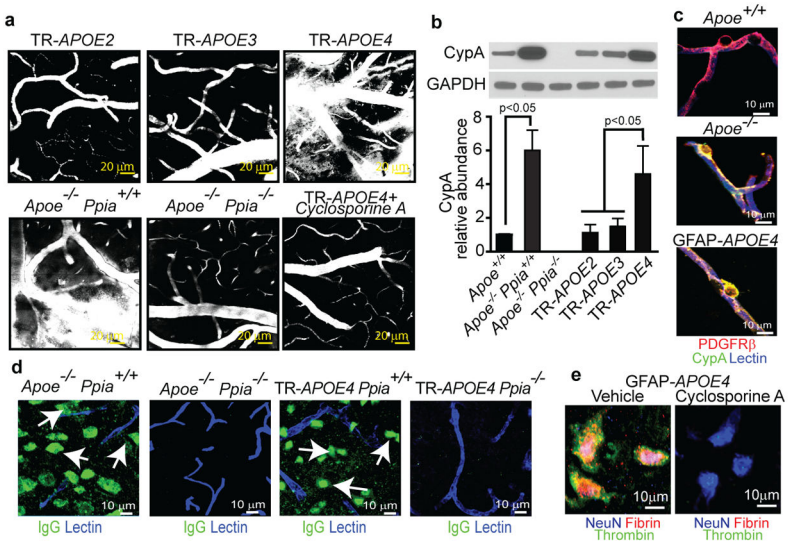

Figure 1. CypA deficiency or inhibition reverses BBB breakdown in *Apoe*$^{-/-}$ and *APOE4* mice

(**a**) Multiphoton microscopy of TMR-Dextran (white) in 6-month-old TR-*APOE2*, TR-*APOE3*, TR-*APOE4*, *Apoe*$^{-/-}$ *Ppia*$^{+/+}$, *Apoe*$^{-/-}$ *Ppia*$^{-/-}$ and cyclosporine A-treated TR-*APOE4* mice. Bar=20 mm. (**b**) CypA immunobloting in brain microvessels from apoE transgenic mice. (**c**) CypA (green) colocalization with PDGFRb-positive pericytes (red; yellow, merged) in hippocampal microvessels from *Apoe*$^{+/+}$, *Apoe*$^{-/-}$ and GFAP-*APOE4* mice. Blue, lectin-positive endothelium. Bar=10mm. (**d**) IgG neuronal uptake (green; lectin-positive vessels, blue) in *Apoe*$^{-/-}$ *Ppia*$^{+/+}$, *Apoe*$^{-/-}$ *Ppia*$^{-/-}$, TR-*APOE4 Ppia*$^{+/+}$ and TR-*APOE4 Ppia*$^{-/-}$ mice. (**e**) Fibrin (red) and thrombin (green) in NeuN-positive neurons (blue) in the hippocampus of 9-month-old GFAP-*APOE4* mice untreated and cyclosporine A-treated. a and c–e, representative results from 4–6 experiments. Scale bar, 10 µm.

NIH-PA Author Manuscript
NIH-PA Author Manuscript
NIH-PA Author Manuscript

NIH-PA Author Manuscript
NIH-PA Author Manuscript
NIH-PA Author Manuscript

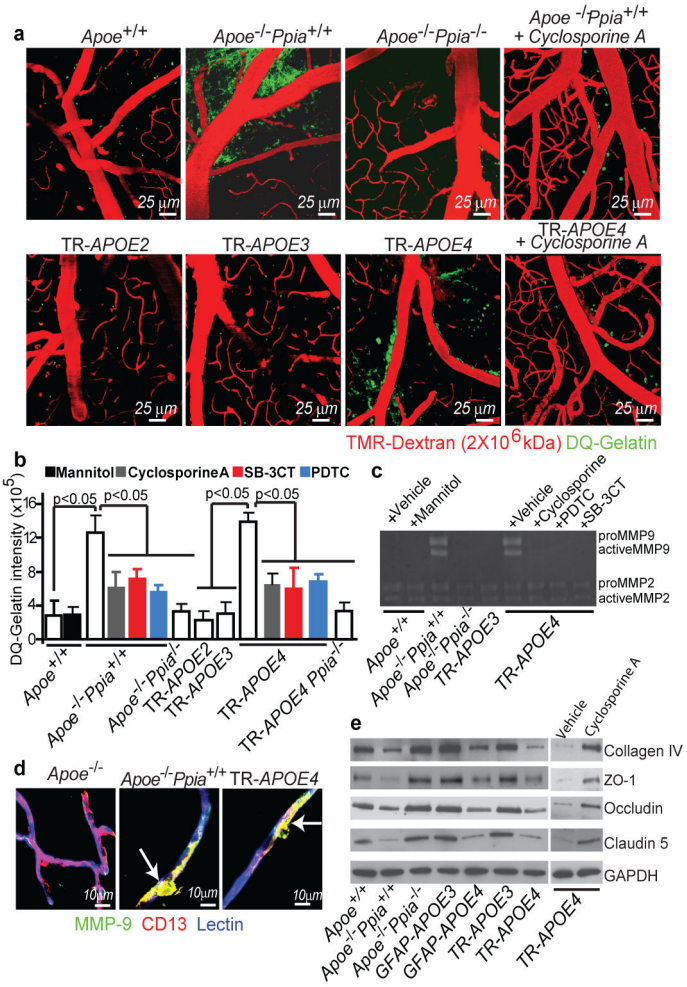

Figure 2. CypA activates NF-kB-MMP-9 pathway causing BBB breakdown in *Apoe*$^{-/-}$ and *APOE4* mice

(**a**) Multiphoton microscopy of DQ-gelatin (green) in 8–9-month-old control, *Apoe*$^{-/-}$ *Ppia*$^{+/+}$, *Apoe*$^{-/-}$ *Ppia*$^{-/-}$, TR-*APOE2*, TR-*APOE3*, TR-*APOE4* and cyclosporine A-treated *Apoe*$^{-/-}$ *Ppia*$^{+/+}$ and TR-*APOE4* mice. Red, cortical vessels. **(b)** Quantification of DQ-gelatin signal in apoE transgenic mice. Effects of cyclosporine A, PDTC, SB-3CT and CypA deletion in *Apoe*$^{-/-}$ and TR-*APOE4* mice. Mean±s.e.m., n=3–6 animals per group.(**c**) Gelatin zymography of brain tissue in control, *Apoe*$^{-/-}$ *Ppia*$^{+/+}$, *Apoe*$^{-/-}$ *Ppia*$^{-/-}$, TR-*APOE3* and TR-*APOE4* mice treated with vehicle, cyclosporine A, PDTC or SB-3CT. (**d**) MMP-9 (green) colocalization with CD13-positive pericytes (red; yellow, merged) in cortical microvessels from 9-month-old *Apoe*$^{+/+}$*Ppia*$^{+/+}$, *Apoe*$^{-/-}$ *Ppia*$^{+/+}$ and TR-*APOE4* mice. Blue, lectin-positive endothelium. Bar=10 mm. (**e**) Reduced collagen-IV, ZO-1, occludin and claudin-5 levels in 2-week-old *Apoe*$^{-/-}$ and TR-*APOE4* mice and reversal by CypA ablation (*Apoe*$^{-/-}$ *Ppia*$^{+/+}$) and cyclosporine A (TR-*APOE4*). c and e, representative results from 4–6 experiments.

NIH-PA Author Manuscript

NIH-PA Author Manuscript

NIH-PA Author Manuscript

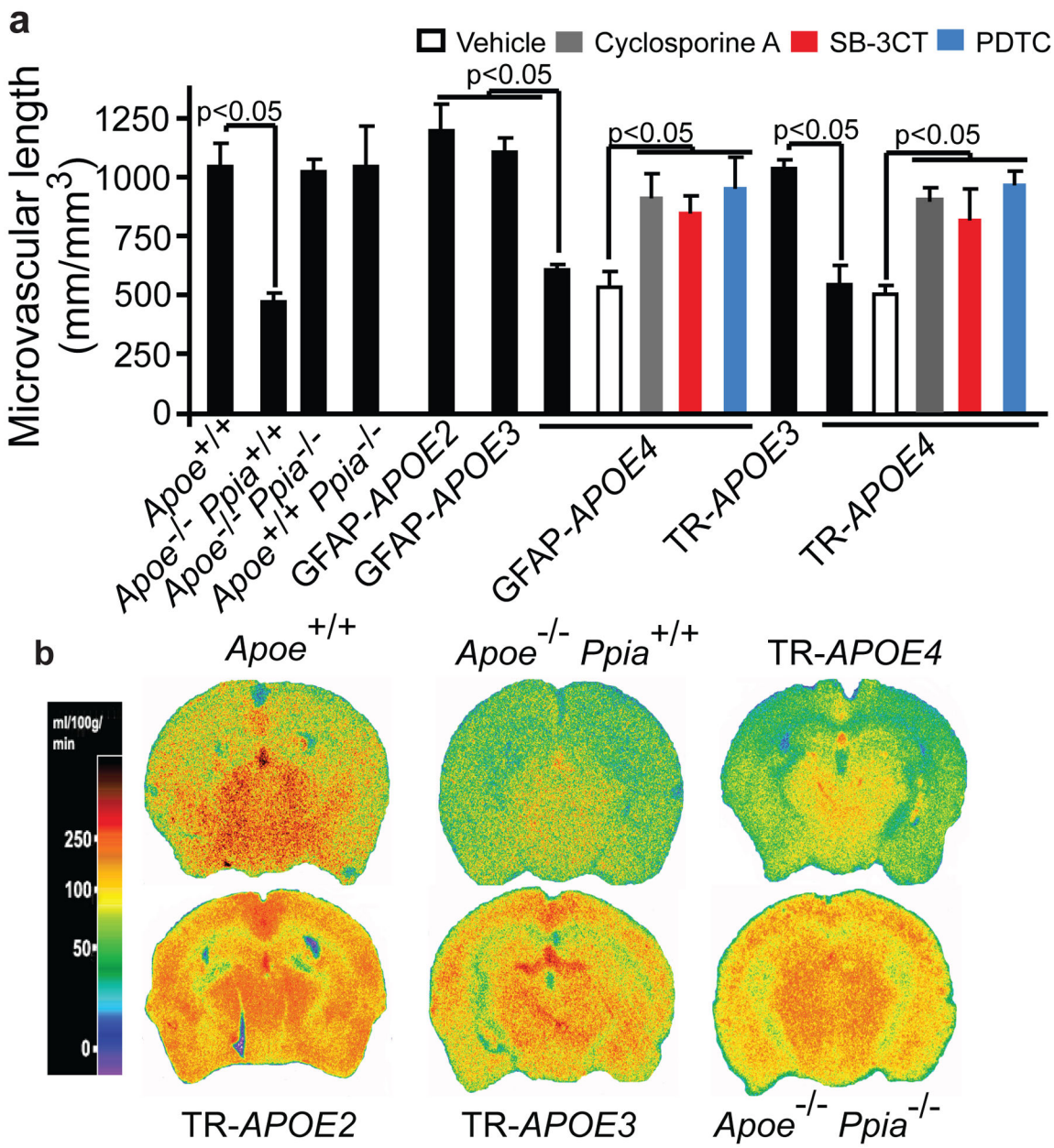

Figure 3. CypA ablation or inhibition reverses microvascular and CBF reductions in *Apoe*$^{-/-}$ and *APOE4* mice

(**a**) Capillary length in the hippocampus of apoE transgenic mice including *Apoe*$^{-/-}$ *Ppia*$^{+/+}$, *Apoe*$^{-/-}$ *Ppia*$^{-/-}$ and GFAP-*APOE4* and TR-*APOE4* mice treated with cyclosporine A, SB-3CT or PDTC (mean±s.e.m., n=5 animals per group). (**b**) ^{14}C-iodoantipyrine CBF autoradiograms in 9-month-old transgenic apoE mice. b, representative results from 6 experiments.

NIH-PA Author Manuscript

NIH-PA Author Manuscript

NIH-PA Author Manuscript

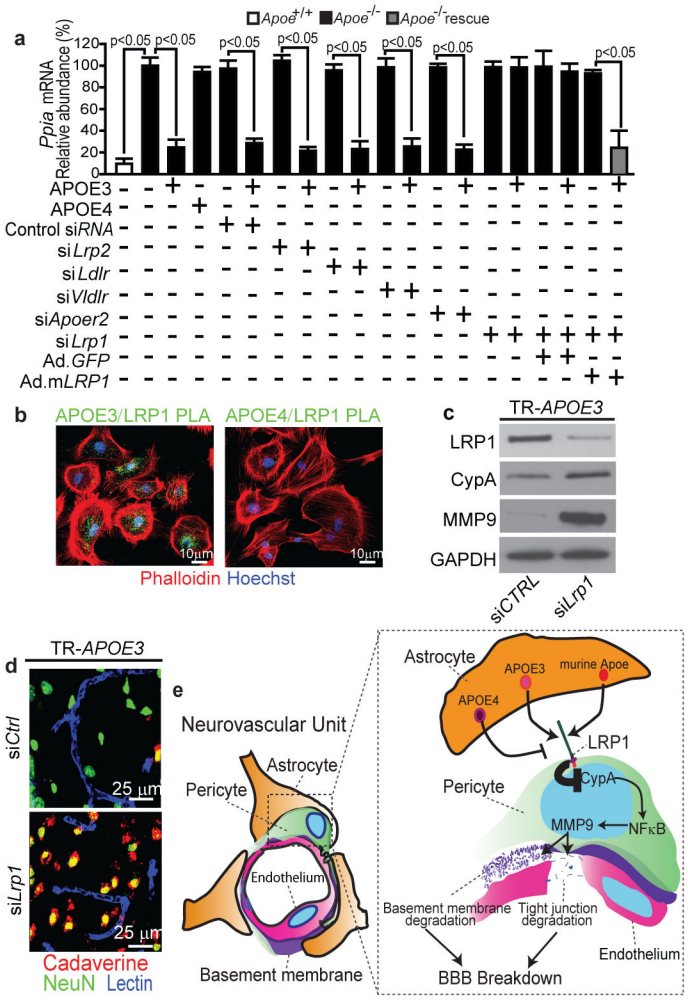

Figure 4. ApoE isoform-specific regulation of CypA-NF-kB-MMP-9 pathway in pericytes

(**a**) CypA mRNA quantification in *Apoe*$^{-/-}$ pericytes after treatment with astrocyte-secreted apoE3, apoE4, si*RNA* silencing of LDL/apoE receptors and adenoviral-mediated re-expression of LRP1 minigene (Ad.m *LRP1*). Mean±s.e.m., n=3 independent cultures. (**b**) Proximity ligation imaging of apoE3 and apoE4 interaction with LRP1. (**c–d**) LRP1, CypA and MMP-9 immunodetection (**c**) and neuronal uptake (NeuN, green) of cadaverine-Alexa-Fluor-555 (red; yellow, merged) (**d**) in the hippocampus of 6-month-old GFAP-*APOE3* mice after si*LRP1* or control si*RNA* infusion. Blue, lectin-positive capillaries. (**e**) A schematic showing that astrocyte-secreted apoE3 and murine apoE, but not apoE4, signal to pericytes via LRP1 suppressing the CypA-NF-kB-MMP-9 pathway that causes BBB breakdown. b and c–d, representative results from 6 experiments.

NIH-PA Author Manuscript
NIH-PA Author Manuscript
NIH-PA Author Manuscript

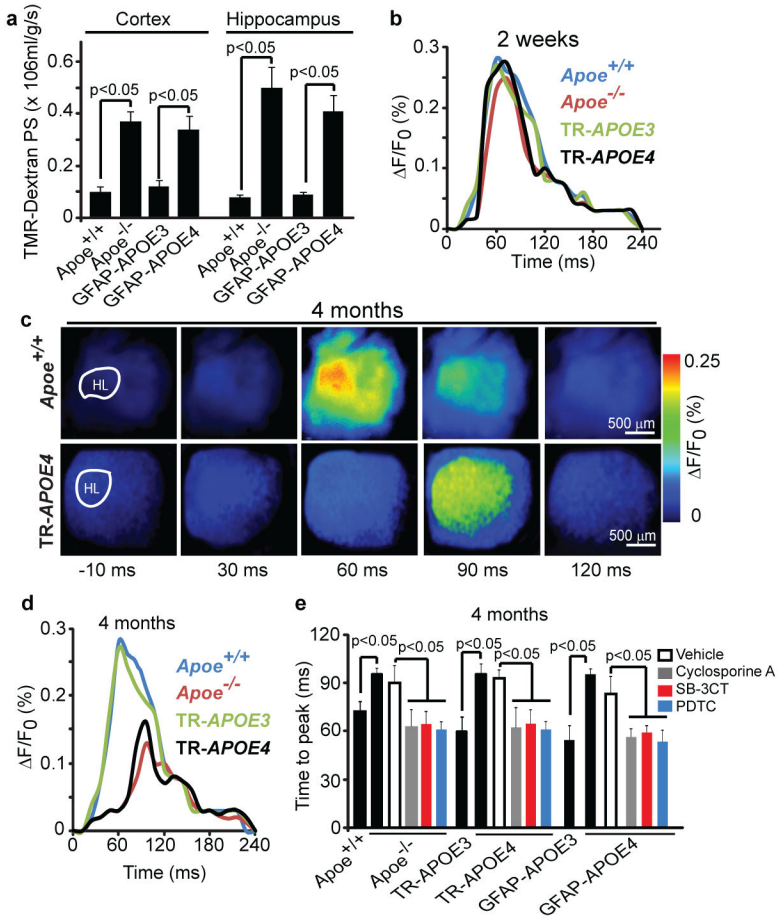

Figure 5. Vascular defects in *Apoe*$^{-/-}$ and *APOE4* mice precede neuronal dysfunction

(**a**) The blood-brain barrier permeability surface (PS) product for tetramethylrhodamine (TMR)-dextran (40,000 Da) in the cortex and hippocampus of 2-week-old *Apoe*$^{+/+}$, *Apoe*$^{-/-}$, GFAP-*APOE3* and GFAP-*APOE4* mice measured by non-invasive fluorescence spectroscopy. (**b**) Representative time-lapse imaging profile analysis of fluorescent voltage sensitive dye (VSD) signal response in the hind-limb somatosensory cortex after stimulation in 2-week-old *Apoe*$^{+/+}$, *Apoe*$^{-/-}$, TR-*APOE3* and TR-*APOE4* mice. (**c**) VSD imaging of cortical responses to hind-limb stimulation in 4-month-old *Apoe*$^{+/+}$ and TR-*APOE4* mice. (**d**) Representative VSD signal responses in the hind-limb somatosensory cortex region after stimulation in 4-month-old *Apoe*$^{+/+}$, *Apoe*$^{-/-}$, TR-*APOE3* and TR-*APOE4* mice. (**e**) Time to peak in fluorescent VSD signal after hind-limb stimulation in 4-month-old *Apoe*$^{+/+}$, *Apoe*$^{-/-}$, TR-*APOE3*, TR-*APOE4*, GFAP-*APOE3* and GFAP-*APOE4* mice and in *Apoe*$^{-/-}$, TR-*APOE4* and GFAP-*APOE4* mice treated with cyclosporine A, SB-3CT, PDTC or vehicle. a and e, mean±s.e.m., n= 5 animals per group.